

# Structure of cosmic strings for a gauged $B - L$ symmetry and two Higgs fields

José Antonio García-Hernández, Victor Muñoz-Vitelly  
and Wolfgang Bietenholz

Instituto de Ciencias Nucleares  
Universidad Nacional Autónoma de México  
A.P. 70-543, C.P. 04510 Ciudad de México, Mexico

In the Standard Model, the difference between the baryon number  $B$  and the lepton number  $L$  is conserved, which represents a symmetry that is global and exact, and therefore unnatural. We turn it into a naturally exact, local symmetry by coupling the quantum number  $B - L$  to an Abelian gauge field. Gauge anomalies are cancelled by adding right-handed neutrinos  $\nu_R$ , which are not sterile in this case. Therefore the usual Majorana term is forbidden by gauge symmetry, but we arrange for a  $\nu_R$ -mass by adding a Higgs-type 1-component complex scalar field. Thus we arrive at a modest, well-motivated extension of the Standard Model.

In this framework, we investigate the field equations in the extended gauge-Higgs sector, involving both Higgs fields and the non-standard  $U(1)$  gauge field. They are given by a set of coupled, non-linear differential equations, which we solve numerically, focusing on the structures of cosmic strings. For a variety of parameters, we identify the string profiles and energy densities, assuming appropriate boundary conditions. In particular, these profiles depend on the winding number of each of the Higgs fields. As an amazing peculiarity, we discover — for high winding numbers — “overshooting” and “co-axial” solutions; in the latter case, the profile of the standard Higgs field changes its sign near the core of the cosmic string.

# Contents

<b>1</b>	<b>Motivation</b>	<b>2</b>
<b>2</b>	<b>Cosmic strings</b>	<b>4</b>
2.1	Prototypes . . . . .	5
2.1.1	Global cosmic strings . . . . .	5
2.1.2	Local cosmic strings . . . . .	7
2.2	Formation of cosmic strings . . . . .	8
<b>3</b>	<b>Standard Model extension with a gauged <math>B - L</math> symmetry and massive, right-handed neutrinos</b>	<b>9</b>
3.1	Gauge-Higgs field equations . . . . .	12
<b>4</b>	<b>Cosmic string profiles</b>	<b>14</b>
<b>5</b>	<b>Overview and conclusions</b>	<b>19</b>
<b>A</b>	<b>Numerical methods</b>	<b>22</b>
<b>B</b>	<b>Bound on the mixed term in the Higgs potential</b>	<b>23</b>

## 1 Motivation

The Standard Model of particle physics is extremely successful: its predictions have been confirmed over and over again, to higher and higher precision. Yet, there are reasons not to be completely satisfied with it: of course, it does not include gravity, Dark Matter and Dark Energy. However, in this work we take an intrinsic, conceptual shortcoming as our point of departure: the exact conservation of the difference between the baryon number  $B$  and lepton number  $L$ . The Standard Model allows for individual changes of  $B$  and of  $L$ , due to topological windings in the  $SU(2)_L$  gauge field. However, the theoretical transition rate is extremely low (at accessible energies), hence  $B$  and  $L$  number violations have never been observed.

On the other hand, the conservation of the difference  $B - L$  is theoretically exact, as reflected by the property that the baryon current  $J_\mu^B$  and the lepton

current  $J_\mu^L$  have the same divergence,

$$\partial^\mu J_\mu^B = \partial^\mu J_\mu^L = -\frac{N_g}{16\pi^2} \text{Tr}[W^{\mu\nu} \tilde{W}_{\mu\nu}] , \quad (1.1)$$

where  $N_g$  is the number of fermion generations, while  $W^{\mu\nu}$  and  $\tilde{W}_{\mu\nu} = \frac{1}{2}\epsilon_{\mu\nu\rho\sigma}W^{\rho\sigma}$  are the  $SU(2)_L$  field strength tensor and its dual, see *e.g.* Ref. [1].

Hence  $B - L$  conservation represents an exact, global symmetry of the Standard Model,  $\partial^\mu(J_\mu^B - J_\mu^L) = 0$ . This seems unnatural: global symmetries are usually just approximately valid in some energy regime — in general, there is no reason for them to be exact. Another exception within the Standard Model is Lorentz invariance, which — along with locality — also implies CPT symmetry [2]. However, from the perspective of General Relativity, Lorentz invariance can be interpreted as a gauge symmetry, so from that point of view its exactness is natural and necessary.

In this work, we refer to the analogous scenario for the  $B - L$  invariance, which we turn into a (local) gauge symmetry. So we step beyond the Standard Model, but in a controlled and economic manner, by adding only few fields, for which there is a crystal-clear motivation.

First, this means that we couple the charge  $B - L$  to an Abelian gauge field  $\mathcal{A}_\mu$ , which explains its conservation. The Higgs mechanism will arrange for this gauge field to be heavy, thus avoiding long-range effects and therefore also avoiding obvious contradictions with observations. This addition alone leads to gauge anomalies, due to the unbalance between the left- and right-handed fermion content of the Standard Model. This is fixed by adding a right-handed neutrino  $\nu_R$  to each fermion generation (our notation does not distinguish its flavor).

Usually, this addition provides a Majorana mass term, which is, however, forbidden in this scenario, because here such a term has a gauge charge  $B - L = -2$ . Conceptually, it is not strictly required to obtain a mass for the right-handed neutrino. Still, we consider it well motivated to enable such a mass, by means of an extra Higgs-type field  $\chi$ . Its form is again minimal, just a 1-component, complex scalar field. These are all the ingredients that we add to the Standard Model.

Within this gauge-Higgs sector, we study the field equations, which can be solved numerically. We are interested in vortices in the  $\mathcal{A}_\mu$  configurations as topological defects, and the resulting non-standard cosmic strings. For a variety of sectors in parameter space, we explore the radial profile functions of such local cosmic strings, and their dependence on the winding numbers

of both Higgs fields (standard and non-standard). We present a set of solutions, which are not ruled out by observations; this statement includes recent bounds based on gravitational waves [3, 4]. Hence such cosmic strings could have persisted since the early Universe, along the lines suggested in Refs. [5], and reviewed *e.g.* in Refs. [6] (though these references mostly refer to standard cosmic strings<sup>1</sup>).

As an interesting peculiarity, we identify an extreme region in parameter space where solutions emerge that we denote as “overshooting” and “co-axial” strings. “Overshooting” means that a profile function starts at 0 in the core and exceeds at short distances its asymptotic value far from it. In the co-axial case, the profile function of the standard Higgs field  $\Phi$  changes its sign near the core of the string. Such exotic solutions are hardly known, although this possibility was reported before in Ref. [7], but in a different set-up, without  $(B - L)$ -gauging.

Section 2 reviews some basic aspects of cosmic strings. In Section 3, we explicitly describe the (modestly) extended Standard Model that this work deals with. In particular, Subsection 3.1 discusses the corresponding field equations in the sector composed of the non-standard Abelian gauge field  $\mathcal{A}_\mu$ , as well as the standard and non-standard Higgs field,  $\Phi$  and  $\chi$ . A multitude of numerical solutions, for different action parameters and winding numbers, is presented in Section 4, before arriving at our summary and conclusions in Section 5.

Appendix A adds remarks about the numerical method that we applied to obtain the results in Section 4, including comments on their reliability and precision. Appendix B discusses the conditions for the Higgs-Higgs potential to be bounded from below. Preliminary results of this work were reported before in two theses [8, 9] and a proceeding contribution [10].

## 2 Cosmic strings

Topology plays a relevant role in Quantum Field Theory, for instance the term on the right-hand side of eq. (1.1) represents the topological density (the Chern-Pontryagin density) of a configuration of the gauge field  $W_\mu$  of the weak interaction. Generally, the differentiable configurations of an  $SU(N)$  gauge field ( $N \geq 2$ ) fall into disjoint topological sectors (in four Euclidean

---

<sup>1</sup>Hindmarsh and Kibble also discuss axionic cosmic strings.

dimensions, with suitable boundary conditions), each one characterized by a topological charge  $Q \in \mathbb{Z}$ .

Even when a theory does not have topological sectors from a global perspective, it may still have local topological defects. They are well-known in condensed matter systems, such as type II superconductors [11] (where they lead to Abrikosov strings), non-linear optical systems [12] and superfluid helium  $^4\text{He}$  [13, 14]. Some systems undergo phase transitions, which are related to the percolation of topological defects. This happens in particular in the 2d XY model, where the (un)binding of vortex–anti-vortex pairs drives the Berezinskii-Kosterlitz-Thouless phase transition (for a review, see Ref. [15]). In higher dimensions, *e.g.* in the 3d XY model, such topological defects in 2d sheets tend to pile up to form closed, global strings.

## 2.1 Prototypes

We begin with prototype solutions for global and local cosmic strings, which are inspired by Refs. [6]. The latter will be extended to our system of interest in Section 4.

### 2.1.1 Global cosmic strings

Let us illustrate the concept with the simple case of a complex scalar field  $\chi(x) \in \mathbb{C}$  with the Lagrangian

$$\mathcal{L}(\chi, \partial_\mu \chi) = \frac{1}{2} \partial^\mu \chi^* \partial_\mu \chi - V(|\chi|^2), \quad V(|\chi|^2) = \frac{1}{2} \mu_0^2 |\chi|^2 + \frac{1}{4} \lambda_0 |\chi|^4, \quad (2.1)$$

with  $\lambda_0 > 0$ . For  $\mu_0^2 < 0$ , there is a continuous set of classical vacua, which can be parameterized as

$$\chi_0 = v e^{i\alpha}, \quad v = \sqrt{-\mu_0^2/\lambda_0}, \quad \alpha \in (-\pi, \pi]. \quad (2.2)$$

An obvious ansatz for its generalization to static solutions with non-minimal energies, in cylindrical coordinates ( $r \geq 0$ ,  $\varphi \in (-\pi, \pi]$ ,  $z \in \mathbb{R}$ ), reads

$$\chi(r, \varphi, z) = f(r) e^{in\varphi}, \quad (2.3)$$

where  $f(r) \in \mathbb{R}$  is the *profile function* and  $n \in \mathbb{Z}$  the *winding number*. For the former we impose the boundary conditions  $f(r \rightarrow \infty) = v$ , and — for  $n \neq 0$

—  $f(0) = 0$ , which avoids a phase ambiguity. These boundary conditions are applied when we numerically solve the field equation

$$f''(r) + \frac{1}{r}f'(r) = \left(\frac{n^2}{r^2} + \mu_0^2 + \lambda_0 f^2(r)\right)f(r). \quad (2.4)$$

A prototype solution, for  $n = 1$ , is shown in Figure 1. This plot also shows the radial energy density  $\epsilon(r)$ , which — in this case — is given by

$$\begin{aligned} \epsilon(r) &= \frac{1}{2}|\partial_t\chi|^2 + \frac{1}{2}|\partial_r\chi|^2 + \frac{1}{2r^2}|\partial_\varphi\chi|^2 + \frac{1}{2}|\partial_z\chi|^2 + V(|\chi|^2) \\ &= \frac{1}{2}(\partial_r f)^2 + \frac{1}{2}\left(\frac{1}{r}nf\right)^2 + \frac{1}{2}\mu_0^2 f^2 + \frac{1}{4}\lambda_0 f^4, \end{aligned} \quad (2.5)$$

where we used the properties that this solution is static and constant in  $z$ . In the limits  $r \ll 1$  and  $r \gg 1$  the solution can be expanded analytically in terms of Bessel functions, in agreement with Figure 1 [9].

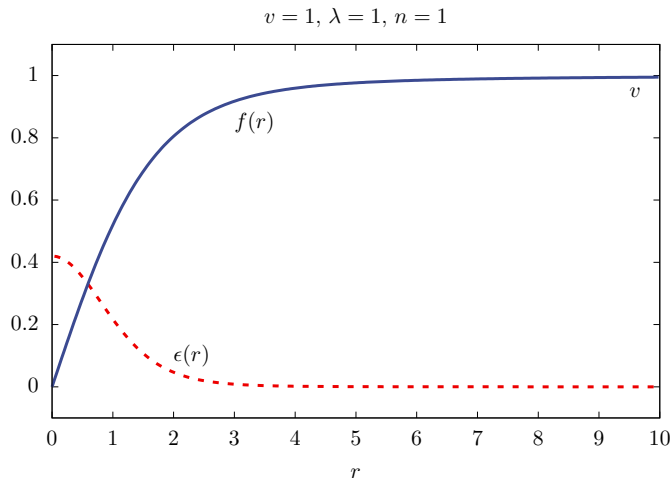


Figure 1: A prototype profile function  $f(r)$  of a global cosmic string, with a topological defect at  $r = 0$ , and  $f(r \rightarrow \infty) = v$ , in cylindrical coordinates, which is obtained by numerically solving eq. (2.4). Here we set  $\lambda_0 = 1$  and introduce dimensionless units by further setting  $v = 1$ , which implies  $\mu_0^2 = -v^2\lambda_0 = -1$ . This example refers to winding number  $n = 1$ . The energy density  $\epsilon(r)$  is computed according to eq. (2.5) up to an additive constant; it decays rapidly as  $r$  increases.

### 2.1.2 Local cosmic strings

Since our study is going to address local cosmic strings, we extend our prototype accordingly, by coupling the scalar field  $\chi$  to a U(1) gauge field  $A_\mu$ .<sup>2</sup> Thus the Lagrangian (2.1) turns into

$$\begin{aligned} \mathcal{L}(\chi, A_\mu) &= \frac{1}{2}(D^\mu\chi)^*(D_\mu\chi) - V(|\chi|) - \frac{1}{4}F^{\mu\nu}F_{\mu\nu} , \\ \text{where} \quad D_\mu\chi &= (\partial_\mu + igA_\mu)\chi , \quad F_{\mu\nu} = \partial_\mu A_\nu - \partial_\nu A_\mu , \end{aligned} \quad (2.6)$$

where  $g$  is the gauge coupling. Now the field equations take the form of two coupled, non-linear differential equations,

$$\begin{aligned} \left( D^\mu D_\mu + \mu_0^2\chi + \lambda_0|\chi|^2 \right)\chi &= 0 , \\ D^\mu F_{\mu\nu} + \frac{ig}{2}\left( (D_\nu\chi)^*\chi - \chi^*D_\nu\chi \right) &= 0 . \end{aligned} \quad (2.7)$$

We stay with the cylindrical ansatz (2.3) and add an ansatz for the configuration of  $A_\mu$ , with  $A_z = 0$ . We fix the gauge such that  $A_0 = A_r = 0$ , *i.e.* there is only a component in the direction of the tangential unit vector  $\hat{\varphi}$ ,

$$\chi(r, \varphi, z) = f(r)e^{in\varphi} , \quad \vec{A}(r, \varphi, z) = \frac{a(r)}{r}\hat{\varphi} . \quad (2.8)$$

This ansatz extends the differential equation (2.4) to

$$\begin{aligned} f'' + \frac{1}{r}f' - \frac{1}{r^2}(n + ga)^2 - \mu_0^2f - \lambda_0f^3 &= 0 , \\ a'' - \frac{1}{r}a' - g(n + ga)f^2 &= 0 . \end{aligned} \quad (2.9)$$

Ansatz (2.8) requires  $a(0) = 0$ , and — as in Subsection 2.1.1 — any winding number  $n \neq 0$  also implies  $f(0) = 0$ . At asymptotically large  $r$ , constant solutions are assumed with  $a(r \rightarrow \infty) = -n/g$  and (as in the case of the global string)  $f(r \rightarrow \infty) = v = \sqrt{-\mu_0^2/\lambda_0}$ .

Again the cases of small and large  $r$  can be analyzed analytically [9], in agreement with the numerical solution shown for a local prototype in Figure 2. In this case, the energy density is given by

$$\epsilon(r) = \frac{1}{2}|\partial_r\chi|^2 + \frac{1}{2}\left| \frac{1}{r}\partial_\varphi\chi + \frac{ig}{r}a\chi \right|^2 + \frac{1}{4}F^{\mu\nu}F_{\mu\nu} + V(|\chi|) . \quad (2.10)$$

---

<sup>2</sup>In the literature, this is known as an “Abelian Higgs model”, which allows for the formation of “Nielsen-Olesen strings”.

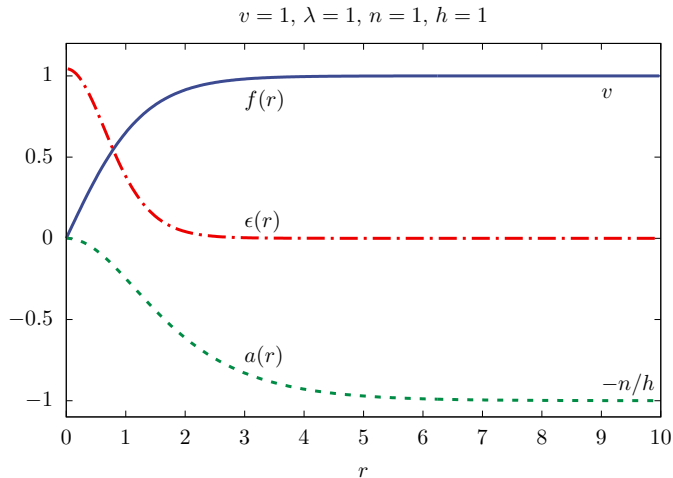


Figure 2: Profile functions  $f(r)$  and  $a(r)$  of a prototype local cosmic string, with a topological defect at  $r = 0$ , in cylindrical coordinates, obtained by numerically solving eqs. (2.9). As in Figure 1, we set  $\lambda_0 = 1$  and  $v = 1$ , which implies  $\mu_0^2 = -1$ , and we refer to the winding number  $n = 1$ . The energy density  $\epsilon(r)$ , given in eq. (2.10), exceeds in the core the value of our global prototype string due to the gauge field contributions.

Interestingly, the string’s energy per length in the  $z$ -direction,  $E/z$ , which is obtained by integrating over the  $(R, \varphi)$ -plane up to a large radius  $R$  (with a regularization in the core), diverges logarithmically for the global string,  $E/z \propto \ln R$ . In contrast,  $E/z$  remains finite for a local string [6].

## 2.2 Formation of cosmic strings

Cosmic strings could be present throughout the Universe, according to the mechanism suggested by Kibble [5]. At the high energies of the Early Universe, topological defects were naturally omnipresent. Under rapid cooling, part of them might have persisted, although they would not be expected in a thermalized low-energy world.

At less than  $10^{-12}$  sec after the Big Bang, the temperature was above 160 GeV, and the electroweak interaction dominated. This period ended when the Higgs field  $\Phi(x) \in \mathbb{C}^2$  acquired a non-zero vacuum expectation value,  $|\langle \Phi \rangle| > 0$ . Well separated regions were causally disconnected, hence in such regions the complex phases of  $\Phi(x)$  could not be correlated. According to Kibble, vortices could have emerged in the interfaces between such regions.



The phase change — integrated over a closed loop within such a surface, around a vortex — amounted to a non-zero, integer multiple of  $2\pi$ . Vortices or anti-vortices naturally pile up to form strings, which may have led to a network of cosmic strings, as discussed *e.g.* in Ref. [16]. Later they might have lost some energy through particle emission or gravitational radiation, but their topological structure could have stabilized them on long term [17], to this day.

In the context of superfluid  $^4\text{He}$ , where vortex lines behave like Abrikosov strings [13], this evolution is known as the Kibble-Zurek mechanism [18], which has been experimentally observed [14]. However, the existence of cosmic strings in the Universe is not confirmed by observations so far; bounds are set based on the Cosmic Microwave Background [19–21] and lately on gravitational wave detections [3, 4]. Numerical studies of the Kibble-Zurek mechanism, by means of Monte Carlo simulations, were conducted in the XY model in  $d = 2$  [22] and in  $d = 3$  [23] spatial dimensions.

### 3 Standard Model extension with a gauged $B - L$ symmetry and massive, right-handed neutrinos

Let us present the building blocks of the model under consideration, in particular its extensions beyond the Standard Model.

As we anticipated in Section 1, our point of departure is promoting  $B - L$  invariance to a gauge symmetry, by coupling the charge  $B - L$  to an Abelian gauge group  $U(1)_{Y'}$ , where  $Y'$  takes a role analogous to the Standard Model weak hypercharge  $Y$ . We denote the gauge field that corresponds to  $U(1)_{Y'}$  by  $\mathcal{A}_\mu$ , cf. Section 1. It is coupled to a linear combination of the conserved charges  $Y$  and  $B - L$ , which we write in the form

$$Y' = 2hY + \frac{1}{2}h'(B - L) , \quad (3.1)$$

where we have introduced the coupling constants  $h$  and  $h'$  (the coefficients 2 and  $1/2$  will turn out to be convenient).

Once this additional gauge field is present, we have to worry about gauge anomalies. As long as we deal with the gauge charges of the Standard Model, there are no such anomalies, but now we have the additional charge  $B - L$ ,

which couples to  $\mathcal{A}_\mu$ , so an anomaly emerges due to the divergence

$$\begin{aligned} \partial^\mu J_\mu^{B-L} &\propto N_g \mathcal{F}^{\mu\nu} \tilde{\mathcal{F}}_{\mu\nu} \\ \mathcal{F}_{\mu\nu} &= \partial_\mu \mathcal{A}_\nu - \partial_\nu \mathcal{A}_\mu, \quad \tilde{\mathcal{F}}_{\mu\nu} = \frac{1}{2} \epsilon_{\mu\nu\rho\sigma} \mathcal{F}^{\rho\sigma}. \end{aligned} \quad (3.2)$$

In fact, for the model that we have assembled so far, this current is anomalous: in each fermion generation, we have an electrically charged lepton with both chiralities, plus a left-handed neutrino, which sum up to  $L = 3$ , with a left-handed dominance. The quarks, however, contribute two flavors with both chiralities, 3 colors and  $B = 1/3$ , which leads to  $B = 4$ , with balanced chiralities.

The overall balance between left and right chiralities can be attained by adding a right-handed neutrino  $\nu_R$  to each fermion generation. Then we obtain  $L = 4$  in each generation, and the divergence of the current in eq. (3.2) vanishes,  $\partial^\mu J_\mu^{B-L} = 0$ . Since  $\nu_R$  is neutral with respect to the gauge charges of the Standard Model, it does not lead to any gauge anomalies involving other gauge fields either.

Now we can build a neutrino mass with a usual Yukawa term, by coupling left-handed and right-handed neutrino fields to the standard Higgs field. Again as usual, this also allows for generation mixing due to the Pontecorvo-Maki-Nakagawa-Sakata matrix. Thus our model is compatible with the observed neutrino oscillation.

On the other hand, in contrast to the usual situation, we cannot add a Majorana mass term for  $\nu_R$ , because this term  $\propto (\bar{\nu}_R^T i\sigma_2 \nu_R + \text{c.c.})$  carries the charge  $B - L = -2$ . Still, we consider the model unnatural without a (purely) right-handed neutrino mass term, impeded by the gauge group  $U(1)_{Y'}$ .

The simplest way to incorporate such a mass term is the inclusion of a non-standard Higgs-type field, which is just a 1-component, complex scalar field  $\chi(x) \in \mathbb{C}$ , carrying the quantum number  $B - L = 2$ . This scalar field enables a term of the type  $\chi \nu_R^T i\sigma_2 \nu_R + \text{c.c.}$  in one generation. For several generations another mixing is possible, in addition to the Pontecorvo-Maki-Nakagawa-Sakata mixing.

The field  $\chi$  naturally has a Lagrangian with a quartic potential, just as in eq. (2.1), which keeps it power-counting renormalizable. Moreover, the standard Higgs field  $\Phi \in \mathbb{C}^2$  and the non-standard Higgs field  $\chi \in \mathbb{C}$  (both with dimension mass) can also contribute a combined, gauge invariant, quartic term  $\propto \Phi^\dagger \Phi \chi^* \chi$ .

So we have added the fields  $\mathcal{A}_\mu$ ,  $\nu_R$  and  $\chi$  to the Standard Model, which leads to a consistent, well-motivated model, and we won't add anything more. Still, we will occasionally refer to the scenario where this model is part of a Grand Unified Theory (GUT). Since its gauge group  $SU(3)_c \otimes SU(2)_L \otimes U(1)_Y \otimes U(1)_{Y'}$  has rank 5, the GUT gauge group cannot be  $SU(5)$ , so the simplest candidate is  $SO(10)$  [24]. In contrast to  $SU(5)$ , the  $SO(10)$  GUT is not ruled out by the lower bound for the proton lifetime of about  $10^{32}$  years. In this theory, the non-standard hypercharge  $Y'$ , as a linear combination of  $Y$  and  $B - L$ , takes the specific form [25]

$$Y' = Y - \frac{5}{4}(B - L) . \quad (3.3)$$

Thus it fulfills the orthogonality condition  $\sum_f Y_f Y'_f = 0$ , as well as the normalizations  $\sum_f Y_f^2 = 10/3 N_g$ ,  $\sum_f Y_f'^2 = 5 N_g$ , where  $N_g$  is again the number of fermion generations, and the sums run over all fermions. In the numerical analysis of Section 4, we are going to pay attention to the specific form of  $Y'$  given in eq. (3.3), with  $h'/h = -5$ .

A study of the field equations of this extended Standard Model, in its complete form, is beyond the scope of this work. Here we focus on its gauge-Higgs sector involving the fields  $\Phi$ ,  $\chi$  and  $\mathcal{A}_\mu$ , which extends the prototype Lagrangian (2.6) to

$$\mathcal{L} = \frac{1}{2} D^\mu \Phi^\dagger D_\mu \Phi + \frac{1}{2} d^\mu \chi^* d_\mu \chi - V(\Phi, \chi) - \frac{1}{4} \mathcal{F}_{\mu\nu} \mathcal{F}^{\mu\nu} , \quad (3.4)$$

where

$$\begin{aligned} D_\mu \Phi &= \partial_\mu \Phi + ih \mathcal{A}_\mu \Phi , & d_\mu \chi &= \partial_\mu \chi + ih' \mathcal{A}_\mu \chi , \\ V(\Phi, \chi) &= \frac{1}{2} \mu^2 \Phi^\dagger \Phi + \frac{1}{4} \lambda (\Phi^\dagger \Phi)^2 + \frac{1}{2} \mu'^2 \chi^* \chi + \frac{1}{4} \lambda' (\chi^* \chi)^2 \\ &\quad + \frac{1}{2} \kappa \Phi^\dagger \Phi \chi^* \chi . \end{aligned} \quad (3.5)$$

Regarding the covariant derivatives  $D_\mu \Phi$  and  $d_\mu \chi$ , we considered our ansatz (3.1) along with the known charges  $Y_\Phi = 1/2$  and  $(B - L)_\chi = 2$ . On the other hand, in this analysis we do not include the couplings of  $\Phi$  to the Standard Model gauge fields  $SU(2)_L$  and  $U(1)_Y$ , nor its Yukawa couplings.

Hence we do not consider any of the Standard Model gauge or fermion fields, assuming that they do not significantly affect the cosmic string structures to be reported in Section 4.

We are interested in the case where both Higgs fields undergo spontaneous symmetry breaking, at least in the space outside the core of a cosmic string. In particular, this should lead to a mass of the gauge field  $\mathcal{A}_\mu$ ,  $m_{\mathcal{A}} = hv + h'v'$ , which is sufficiently large to explain that this gauge boson has not been observed. We denote the corresponding vacuum expectation values (VEVs) asymptotically far from this core as

$$v = |\langle \Phi(r \rightarrow \infty) \rangle|, \quad v' = |\langle \chi(r \rightarrow \infty) \rangle|. \quad (3.6)$$

Since our analysis will be kept on tree level, we do not keep track of renormalization effects, so the conditions  $v > 0$ ,  $v' > 0$  imply

$$\mu^2 < 0, \quad \mu'^2 < 0, \quad \kappa < \min\left(\frac{\mu^2 \lambda'}{\mu'^2}, \frac{\mu'^2 \lambda}{\mu^2}\right). \quad (3.7)$$

Moreover, for the system to have a ground state, the potential  $V(\Phi, \chi)$  must be bounded from below. This imposes the additional constraints

$$\lambda > 0, \quad \lambda' > 0, \quad \kappa < \sqrt{\lambda \lambda'}. \quad (3.8)$$

The constraints on  $\kappa$  in eqs. (3.7) and (3.8) are not obvious and will be derived in Appendix B. They can be synthesized by the single inequality

$$\kappa^2 < \lambda \lambda'. \quad (3.9)$$

### 3.1 Gauge-Higgs field equations

In accordance with Section 2, we search for static solutions of the field equations, for which we make an ansatz in cylindrical coordinates, as in eq. (2.8),

$$\begin{aligned} \Phi(r, \varphi, z) &= \begin{pmatrix} 0 \\ 1 \end{pmatrix} \phi(r) \exp(in\varphi), \\ \chi(r, \varphi, z) &= \xi(r) \exp(in'\varphi), \\ \vec{\mathcal{A}}(r, \varphi, z) &= \frac{a(r)}{r} \hat{\varphi}. \end{aligned} \quad (3.10)$$

Here  $\phi(r)$ ,  $\xi(r)$  and  $a(r)$  are the radial profile functions of a static field configuration,  $\hat{\varphi}$  is the tangential unit vector, and  $n, n' \in \mathbb{Z}$  are the winding numbers of the standard and non-standard Higgs field, respectively.

This ansatz leads to the Euler-Lagrange field equations

$$\begin{aligned}
\frac{d^2\phi}{dr^2} + \frac{1}{r} \frac{d\phi}{dr} &= \left[ \frac{(n+ha)^2}{r^2} + \mu^2 + \lambda\phi^2 + \kappa\xi^2 \right] \phi, \\
\frac{d^2\xi}{dr^2} + \frac{1}{r} \frac{d\xi}{dr} &= \left[ \frac{(n'+h'a)^2}{r^2} + \mu'^2 + \lambda'\xi^2 + \kappa\phi^2 \right] \xi, \\
\frac{d^2a}{dr^2} - \frac{1}{r} \frac{da}{dr} &= h\phi^2(n+ha) + h'\xi^2(n'+h'a). \tag{3.11}
\end{aligned}$$

Their derivation is non-trivial but straightforward, hence we do not display intermediate steps here; they are documented in detail in Refs. [8, 9].

Before we proceed to the numerical solutions of eqs. (3.11), we still have to specify the boundary conditions for the profile functions. They again generalize the setting of Subsection 2.1.2:

- In the core of the string, at  $r = 0$ , we have to require  $a(0)$  to vanish, as the ansatz (3.10) shows. The same applies to both Higgs fields, but in that case only if the corresponding winding number is non-zero, such that a phase ambiguity has to be avoided. Altogether, the boundary conditions in the core take the form

$$\phi(0) = 0 \quad \text{if } n \neq 0; \quad \xi(0) = 0 \quad \text{if } n' \neq 0; \quad a(0) = 0. \tag{3.12}$$

- Asymptotically far from the string, for  $r \rightarrow \infty$ , we require all three profile functions to be constant in  $r$ . This implies that  $\phi(r \rightarrow \infty)$  and  $\xi(r \rightarrow \infty)$  converge to their VEVs in the absence of a string, *i.e.*  $v$  and  $v'$ , respectively. Eqs. (3.11) show that this limit also relates  $v$  and  $v'$ .

Since these VEVs are independent,  $a(r \rightarrow \infty)$  has to coincide with  $-n/h$  and with  $-n'/h'$ , which imposes an additional relation between the two winding numbers.

To summarize, the asymptotic boundary conditions (in their simplest form) read

$$\begin{aligned}
\phi(r \rightarrow \infty) &= v = \frac{\kappa\mu'^2 - \mu^2\lambda'}{\lambda\lambda' - \kappa^2}, \\
\xi(r \rightarrow \infty) &= v' = \frac{\mu^2\kappa - \mu'^2\lambda}{\lambda\lambda' - \kappa^2}, \\
a(r \rightarrow \infty) &= -\frac{n}{h} = -\frac{n'}{h'}. \tag{3.13}
\end{aligned}$$

The inequalities (3.7) and (3.9) ensure  $v, v' > 0$ .

Usually we will be dealing with dimensionless units. In order to convert them to physical units, we take  $v = 246 \text{ GeV}$  as our reference quantity, which turns all other quantities into physical units as well. In the examples to be reported in Section 4, we consider two values for  $v$ , which convert the distance  $r = 1$  into a physical length as follows:

$$\begin{aligned} v = 0.01 & \quad : \quad r = 1 \text{ corresponds to } 8 \cdot 10^{-6} \text{ fm} \\ v = 0.5 & \quad : \quad r = 1 \text{ corresponds to } 4 \cdot 10^{-4} \text{ fm} . \end{aligned} \tag{3.14}$$

## 4 Cosmic string profiles

We are now going to present numerical solutions for a variety of parameter sets. In all these examples, we set  $\lambda = \lambda' = 1$ ; varying these self-couplings did not lead to particularly instructive insight. Moreover, in all examples except for the very last one, we set  $v' = 1$ . In all the figures, the complete parameter set is given in the plot title.

We start with two cases where only one of the Higgs fields performs a non-trivial winding, *i.e.* either  $n = 0$  or  $n' = 0$ . In these cases, we further set the gauge couplings of the non-winding field to 0. These configurations at  $r = 0$ ,  $\xi(0)$  or  $\phi(0)$  do not need to vanish for  $n' = 0$  or  $n = 0$ , respectively, in agreement with eq. (3.12). This is confirmed by the results shown in Figures 3 and 4, with  $v = 0.5$ .

We proceed to a simple example with windings in both Higgs fields,  $n = n' = 1$ , where now the hierarchy condition is implemented as  $v' = 1 \gg v = 0.01$ . As in the previous examples of Figures 3 and 4, Figure 5 shows smooth and monotonous transitions from  $\phi(0) = \xi(0) = a(0) = 0$  to the asymptotic values given in eq. (3.13). These curves hardly depend on  $\kappa$ , because the potential is strongly dominated by the purely  $\chi$ -dependent terms (note that  $\mu'^2 = -\lambda'v'^2 - \kappa v^2 \approx -\lambda'v'^2$  in this case).

In order to further explore the scenario where the hierarchy  $v < v'$  is not that extreme, we return to the standard Higgs VEV  $v = 1/2$ , as in Figures 3 and 4, while keeping all other parameters unchanged. The outcome is shown in Figure 6. In this case, also the mixed term becomes relevant, as we see from the significant  $\kappa$ -dependence at short distances.

We proceed to the exploration of somewhat exotic scenarios by considering a strong winding in the  $\xi$ -field,  $n' = -5$ . The other parameters and the profiles are given in Figure 7. We see that this leads to a qualitatively new

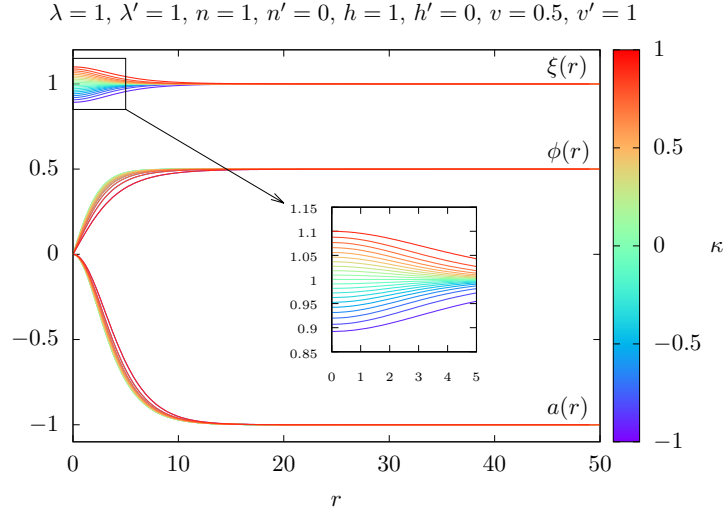


Figure 3: String profiles for the fields  $\phi(r)$ ,  $\xi(r)$  and  $a(r)$  over the range  $|\kappa| < 1$ . Due to  $n' = 0$ ,  $\xi(0)$  does not vanish, but there is still the condition  $\xi'(0) = 0$ .

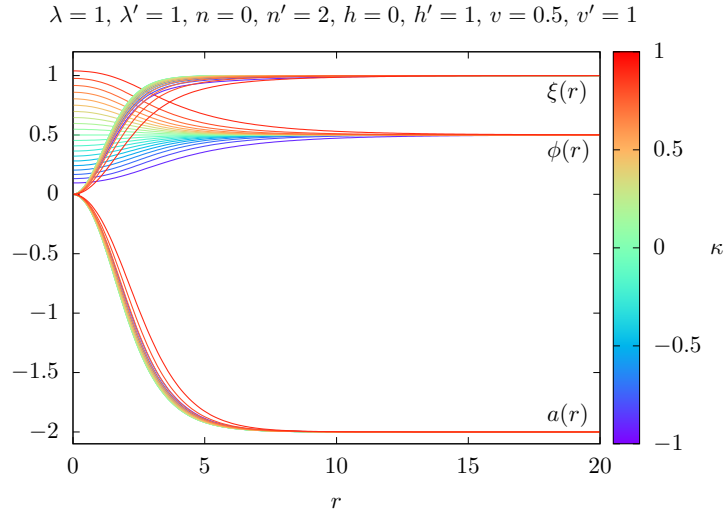


Figure 4: String profiles for the fields  $\phi(r)$ ,  $\xi(r)$  and  $a(r)$  over the allowed range  $|\kappa| < 1$ . Due to  $n = 0$ ,  $\phi(0)$  does not vanish, but there is still the condition  $\phi'(0) = 0$ .

feature: for increasing radius  $r$ , the profile function  $\phi(r)$  *overshoots* its asymptotic value in cases where  $\kappa$  is sufficiently positive. This non-monotonous shape between the known asymptotic values at small and large  $r$  is amaz-

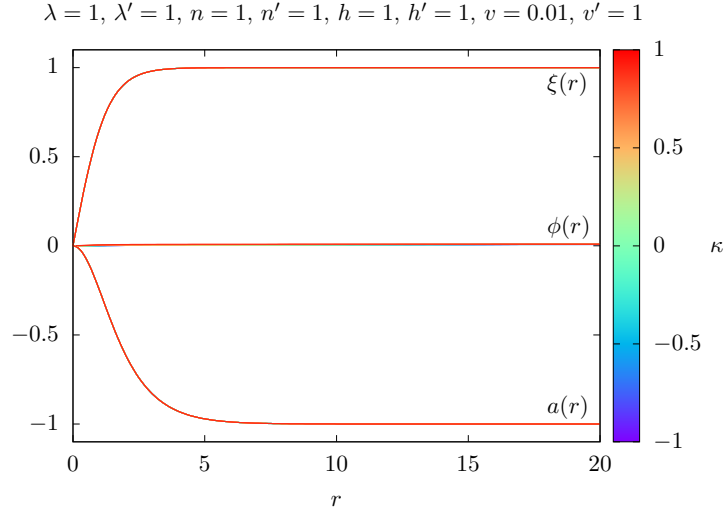


Figure 5: String profiles for the fields  $\phi(r)$ ,  $\xi(r)$  and  $a(r)$  over the range  $|\kappa| < 1$ . We see a smooth and monotonous behavior, similar to the prototype in Figure 2.

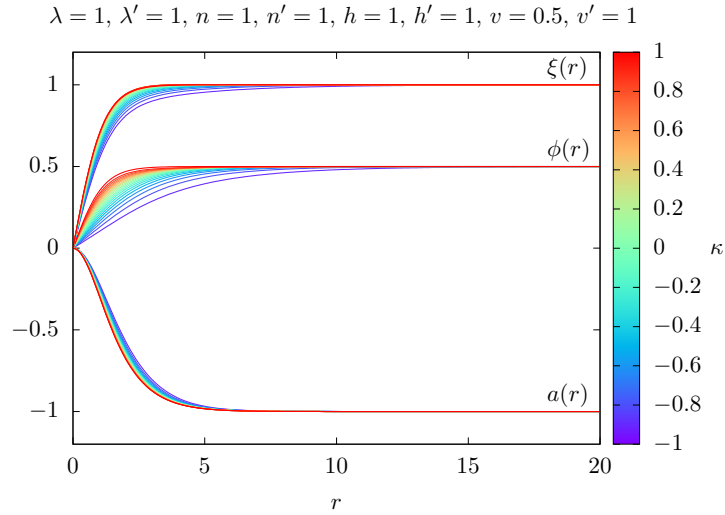


Figure 6: String profiles for the fields  $\phi(r)$ ,  $\xi(r)$  and  $a(r)$  over the range  $|\kappa| < 1$ . The curves are still smooth and monotonous, but we now see a significant dependence on  $\kappa$ .

ing. An elementary particle, which picks up some mass through the standard Higgs mechanism, and which crosses such a cosmic string very close to its core, would temporarily increase its mass. However, even if such cosmic strings exist in the Universe, this event does not seem obvious: with the



scale set according to eq. (3.14), that particle would have to cross the string at a distance  $\lesssim 4 \cdot 10^{-3}$  fm from its core.

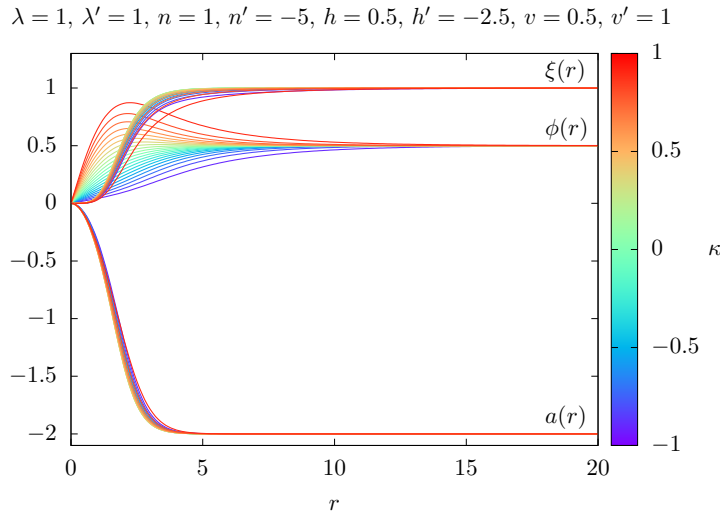


Figure 7: String profiles for the fields  $\phi(r)$ ,  $\xi(r)$  and  $a(r)$  over the range  $|\kappa| < 1$ . For  $\kappa \gtrsim 0$ , we observe that the profile function  $\phi(r)$  *overshoots* its vacuum expectation value in the vicinity of the string core.

We now invert the windings and double their strengths, which yields the profiles in Figure 8. This drives  $a(r \gg 1)$  up to 4, while the overshooting behavior of  $\phi(r)$  at  $\kappa \gtrsim 0$  persists.

Further numerical experiments reveal yet another surprising phenomenon, which is even more exotic. An example is shown in Figure 9, with windings  $n = -2$ ,  $n' = 10$ , and we restore the strong Higgs VEV hierarchy by setting  $v = 0.01$ . In this case, the profile function  $\phi(r)$  is not only non-monotonous, but for certain  $\kappa$  values it is negative at small  $r$ , *i.e.* it actually changes sign near the core. We denote this kind of profile as *co-axial*. It is hardly known that this remarkable behavior is possible, although it was observed before by Bogomol'nyi, in the framework of a standard type of cosmic strings [7]. In his study, he showed that such strings can be unstable; here we leave the question of stability for future investigations. Stability can be explored numerically by means of variational techniques, along the lines of Refs. [7, 26–28].

For that case, Figure 10 shows the radial energy density  $\epsilon(r)$ , which is computed by generalizing eq. (2.10). In contrast to the prototypes in Section 2, it does not monotonously decrease towards 0, but in the co-axial domain it first shoots up before performing its asymptotic decay.

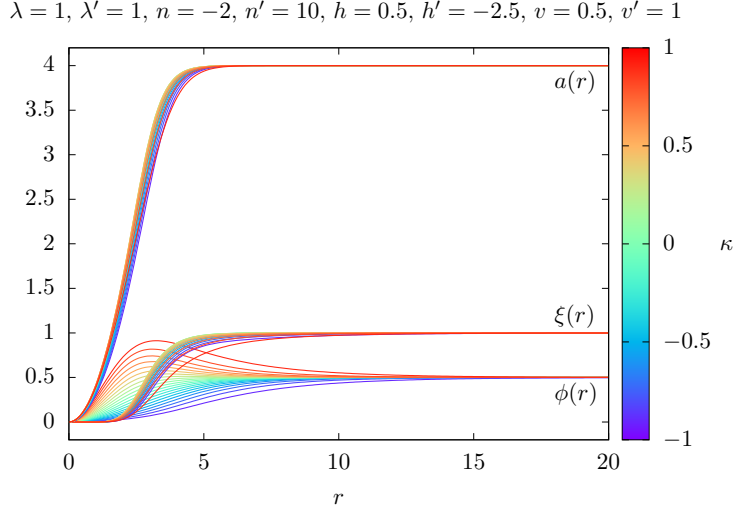


Figure 8: String profiles for the fields  $\phi(r)$ ,  $\xi(r)$  and  $a(r)$  over the range  $|\kappa| < 1$ . As in Figure 7, for  $\kappa \gtrsim 0$ , we observe that the profile function  $\phi(r)$  overshoots its vacuum expectation value in the vicinity of the string core.

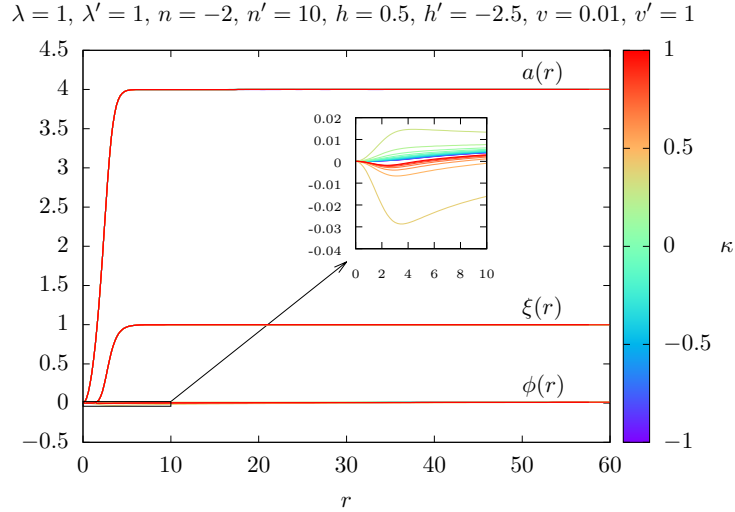


Figure 9: For this parameter set, with the high winding  $n' = 10$ , we obtain a *co-axial* profile  $\phi(r)$ . For  $\kappa < 0.25$ , we observe the typical behavior where  $\phi(r)$  monotonously moves to  $v$ . By gradually increasing  $\kappa$  this profile first overshoots, up to a discontinuity in  $\kappa$  where  $\phi(r)$  flips to a co-axial shape, which means that it takes a sign opposite to  $v$  near the core of the string.

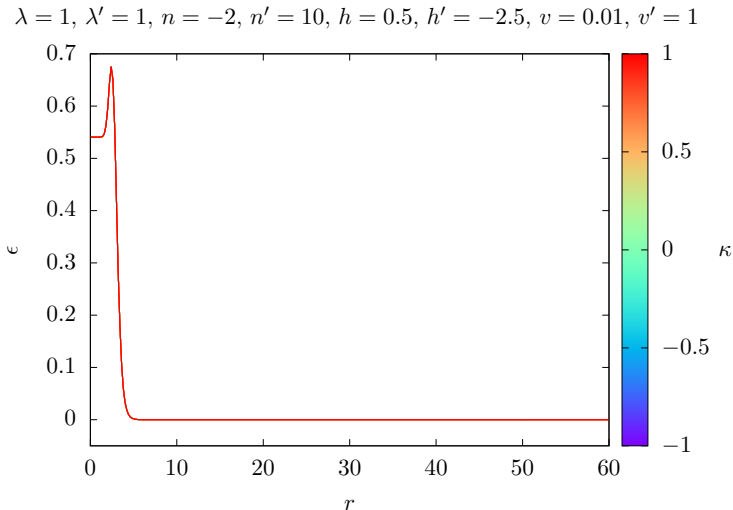


Figure 10: Radial energy density  $\epsilon$  of the solution for the parameters of Figure 9. It is obtained by a straightforward generalization of eq. (2.10). We see a sharp peak in the co-axial regime near the core. In physical units,  $\epsilon = 1$  corresponds to  $4.79 \cdot 10^{19} \text{ GeV}/\text{fm}^3$ .

Let us now address the cases where our model can be embedded in an SO(10) Grand Unified Theory [24], as we announced in Section 3. Relation (3.3), along with the asymptotic conditions for  $a(r)$  given in eq. (3.13), requires

$$\frac{h'}{h} = -5, \quad \frac{n'}{n} = -5. \quad (4.1)$$

In fact, this is the case in the parameter sets of Figures 7, 8, 9 and 10.

At last, we show that also the profile  $\xi(r)$  can overshoot at short distances, as the example in Figure 11 shows.

## 5 Overview and conclusions

We studied a modest and well motivated extension of the Standard Model, where the difference  $B - L$  (baryon number minus lepton number) is turned into the charge of a non-standard U(1) gauge symmetry. In order to cancel gauge anomalies, we added right-handed neutrinos. They obtain a mass by means of an additional 1-component Higgs field.

In the gauge-Higgs sector of this model, which includes the standard and

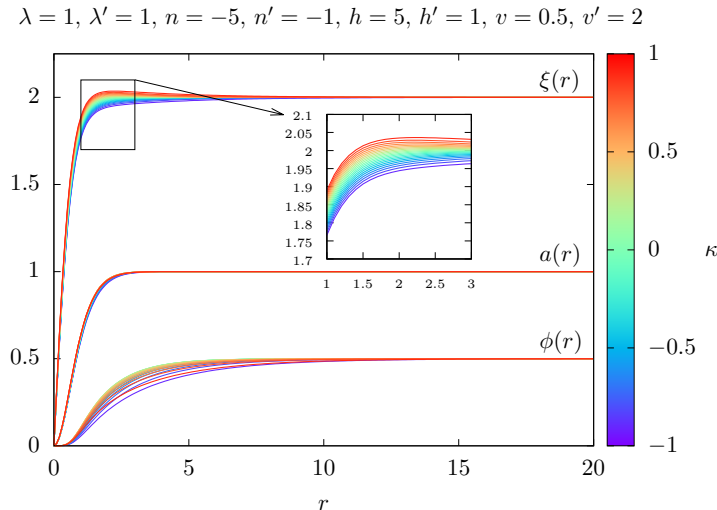


Figure 11: Profile functions for a parameter set which leads to the usual behavior for the profiles  $\phi(r)$  and  $a(r)$ , but a slightly overshooting behavior in this case of the profile function  $\xi(r)$ , around  $r \approx 1.5$ , for  $\kappa \gtrsim 0.6$ .

non-standard Higgs field and the non-standard Abelian gauge field, we studied the possible formation of cosmic strings for a variety of parameters of the Lagrangian and winding numbers of both Higgs fields. Low winding numbers tend to imply smooth and monotonous transitions between the values of the (radial) profile functions in the core and asymptotically far from it. For multiple windings, we observed interesting and amazing effects, in particular the overshooting of the profile function next to the core, and even a co-axial behavior. In some cases, this formulation can be embedded into an SO(10) GUT.

The question of the stability of these solutions to the field equations is left for future investigations, based on a numerical variation study, inspired by Refs. [7, 26–28]. In particular, Ref. [7, 26] observed that Nielsen-Olesen type strings (cf. footnote 2) with  $2\lambda_0/g^2 > 1$  are unstable for winding numbers  $|n| > 1$ . On the other hand, they reported that for  $2\lambda_0/g^2 < 1$  strings with any winding number could be stable, a property which was substantiated in Ref. [27].

For the parameter sets that we studied, the characteristic radius of these strings (the range where the profile function significantly deviates from the asymptotic behavior far from the core) is several orders of magnitude below a nucleon radius. They attain at most  $\mathcal{O}(10^{-3})$  fm; therefore they are good

approximations to 1d “Nambu-Goto strings”.

Regarding the *string tension*, we refer to the example of the co-axial string profile illustrated in Figure 9, and Figure 10 shows the corresponding energy density  $\epsilon$ . The string tension is obtained by (numerically) integrating  $\epsilon$  over the plane perpendicular to the string (at fixed  $z$ -coordinate). This yields the energy per unit length, *i.e.* the string tension,  $\mu \simeq 1.2 \times 10^{10} \text{ GeV}^2$ . It is usual to express this quantity in a dimensionless form, by multiplying with the gravitational constant  $G$ ,

$$G\mu \simeq 8.1 \times 10^{-29} . \quad (5.1)$$

Even if such a string has a length that corresponds to the diameter of the visible Universe, about 28.5 Gpc, its mass is just  $9.5 \times 10^{25} \text{ kg}$ , slightly less than the mass of Neptune.

The methods how to derive observational bounds for cosmic are reviewed *e.g.* in Refs. [29]. In particular, such bounds were obtained from precise data of the Cosmic Microwave Background (CMB). Cosmic strings may have caused 1d discontinuities in the CBM (Kaiser-Stebbins-Gott effect). The direct search for such 1d discontinuities led to a bound around  $G\mu < 4 \times 10^{-6}$  [19]. Statistical methods deal with the angular power spectrum of CMB anisotropies. The analysis of data by the satellites WMAP (Wilkinson Microwave Anisotropy Probe) and SDSS (Sloan Digital Sky Survey) led to a bound of  $G\mu < \mathcal{O}(10^{-7})$  [20]. This magnitude was confirmed by an analysis of Planck2015 data [21].

In recent years, this bound was significantly tightened based on gravitational wave observations, referring specifically to (possible) oscillating loops of cosmic strings: Ref. [30] reports  $G\mu < 1.5 \times 10^{-11}$ , and Ref. [4] even finds — based on the third LIGO-Virgo-KARGA Observing Run —  $G\mu < 4 \times 10^{-15}$ . As an outlook, Ref. [31] predicts that the space-based observatory LISA (Laser Interferometer Space Antenna) will arrive at a sensitivity to cosmic string networks with string tensions  $G\mu < \mathcal{O}(10^{-17})$ . However, even that bound is far from excluding the scenario of this work, as our estimate (5.1) shows. The discrepancy is so strong that we can safely conclude that the other parameter sets considered in this work are not observationally ruled out either, and won’t be excluded in the foreseeable future.

**Acknowledgments:** We thank João Pinto Barros and Uwe-Jens Wiese for inspiring discussions and contributions to this project at an early stage. This

work was supported by UNAM-DGAPA through PAPIIT projects IG100219 and IG100322, and by the Mexican *Consejo Nacional de Humanidades, Ciencias y Tecnologías* (CONAHCYT).

## A Numerical methods

Our standard tool to obtain the solutions presented in Chapter 4 was the Python function `scipy.integrate.solve_bvp`. It applies the damped Newton method to the functions of the radial coordinate  $r$ , which is discretized in equidistant sites  $\vec{r} = (r_0, r_1, \dots, r_N)$ , where we typically used values of  $N$  of order  $\mathcal{O}(1000)$ . We inserted standard discretizations of the first and second derivatives.

The iteration of the straight Newton (or Newton-Raphson) method may fail to converge to the correct solution — or fail to converge at all — if the initial guess is not sufficiently good, which represents a serious problem. Effects like overshooting and oscillations in the iteration process can be reduced by using the *damped* Newton method, which optimizes the modification in the iteration step. This can be done by minimizing the norm of the deviation from an exact solution. Typically, this reduces the modification, which corresponds to the damping effect.

For the initial guess, it turned out to be successful to insert an exponential ansatz, *e.g.* for the standard Higgs profile function it would take the form

$$\phi(r) = (1 - e^{-r/r_0})v , \tag{A.1}$$

where the scale  $r_0$  can be varied (one might start from  $r_0 = 1$ ).

For the generation of a set of solutions with varying parameter  $\kappa$ , the solution for one  $\kappa$ -value is a good ansatz for the next one, which differs only slightly. This procedure also yields the overshooting and co-axial solutions, although the original profile ansatz (A.1) is monotonous.

The solutions were submit to a consistency test by inserting them back into the discretized differential equations. The norm of the deviation from an exact solution was at most of order  $\mathcal{O}(10^{-3})$ . Such values only occurred at small  $r$ , where the system is most delicate. In the range  $r \geq \mathcal{O}(1)$ , the precision improved by further orders of magnitude.

As an alternative, we also implemented a relaxation method, which iteratively applies a local improvement to the approximate solutions; this usually amounts to a local smoothing. Its convergence can be slow, but after a large

number of iterations (up to  $10^7$ ), the results agree with the outcome of the damped Newton method (starting from the same initial guess) within the precision of the consistency test.

Finally, we also run experiments with the 4-point Runge-Kutta method, although it is less appropriate for such boundary value problems. For technical reasons (removable singularities), we cannot start at  $r = 0$ , so we started from  $r_\varepsilon = 0.01$ , set the profile functions at  $r_\varepsilon$  to their theoretical values at  $r = 0$  and treated the first derivatives at  $r_\varepsilon$  as free parameters. Only after fine-tuning them to a precision of  $10^{-7}$  we obtained solutions, which are asymptotically constant as  $r$  becomes large within the range of our plots in Chapter 4. Then they agree again with the solutions obtained by the damped Newton method and the relaxation method. Varying the derivatives at  $r_\varepsilon$ , however, leads to a variety of functions which diverge or oscillate as  $r$  increases.

## B Bound on the mixed term in the Higgs potential

We introduce the notation

$$X = \Phi^\dagger \Phi, \quad Y = \chi^* \chi \tag{B.1}$$

to rewrite the potential in the second line of eq. (3.5) as

$$V(X, Y) = \frac{\mu^2}{2} X + \frac{\mu'^2}{2} Y + \frac{\lambda}{4} X^2 + \frac{\lambda'}{4} Y^2 + \frac{\kappa}{2} XY, \tag{B.2}$$

with  $\mu^2, \mu'^2 < 0$ ;  $\lambda, \lambda' > 0$  and  $X, Y \geq 0$ .

Clearly  $V(0, 0) = 0$ ,  $\lim_{X \rightarrow +\infty} V = \lim_{Y \rightarrow +\infty} V = +\infty$ . The Hessian matrix  $\begin{pmatrix} \lambda/2 & \kappa/2 \\ \kappa/2 & \lambda'/2 \end{pmatrix}$  is constant, and it has the eigenvalues

$$\varepsilon_\pm = \frac{1}{2} \left[ \frac{1}{2}(\lambda + \lambda') \pm \sqrt{\frac{1}{4}(\lambda + \lambda')^2 + \kappa^2 - \lambda\lambda'} \right]. \tag{B.3}$$

The discriminant can be written as  $(\lambda - \lambda')^2/4 + \kappa^2$ , which shows that imaginary eigenvalues are excluded. The above form illustrates that  $\varepsilon_\pm > 0$  holds if

$$\kappa^2 < \lambda\lambda', \tag{B.4}$$

which coincides with the constraint (3.9). In this case, the function is convex everywhere, and thus bounded from below.

There is a unique critical point in the  $(X, Y)$ -plane at

$$(X_0, Y_0) = \frac{1}{\lambda\lambda' - \kappa^2}(\kappa\mu'^2 - \lambda'\mu^2, \kappa\mu^2 - \lambda\mu'^2). \quad (\text{B.5})$$

Due to  $\mu^2, \mu'^2 < 0$ , this point is located in the quadrant  $X, Y \geq 0$  that we are considering (that can be seen from the linear part of  $V(X, Y)$ ). This property is equivalent to condition (3.7). With the constraint (B.4) it is a minimum, which confirms that the potential is bounded from below.

It does not make sense to consider the case  $\kappa^2 = \lambda\lambda'$ , where  $X_0$  and  $Y_0$  diverge, and so do  $v$  and  $v'$ , as eqs. (3.13) show.

For  $\kappa^2 > \lambda\lambda'$ , we obtain  $\varepsilon_- < 0$ , so  $(X_0, Y_0)$  is a saddle point and the potential is not bounded from below. Therefore our numerical study is restricted to  $\kappa$ -values which fulfill the constraint (B.4).

## References

- [1] M.E. Peskin and D.V. Schroeder, *An Introduction to Quantum Field Theory*, Addison Wesley, 1997.
- [2] W. Pauli, On the Conservation of the Lepton Charge, [Nuovo Cimento 6 \(1957\) 204-215](#).  
G. Lüders, Proof of the TCP theorem, [Ann. Phys. \(N.Y.\) 2 \(1957\) 1-15](#).  
R. Jost, Eine Bemerkung zum CTP-Theorem, [Helv. Phys. Acta 30 \(1957\) 409-416](#).
- [3] B.P. Abbott *et al.* (LIGO and Virgo Collaborations), Constraints on cosmic strings using data from the first Advanced LIGO observing run, [Phys. Rev. D 97 \(2018\) 102002](#).
- [4] R. Abbott *et al.* (LIGO Scientific Collaboration, Virgo Collaboration and KAGRA Collaboration), Constraints on Cosmic Strings Using Data from the Third Advanced LIGO-Virgo Observing Run, [Phys. Rev. Lett. 126 \(2021\) 241102](#).
- [5] T.W.K. Kibble, Topology of cosmic domains and strings, [J. Phys. A: Math. Gen. 9 \(1976\) 1387-1398](#); Some implications of a cosmological phase transition, [Phys. Rep. 67 \(1980\) 183-199](#).



- [6] M.B. Hindmarsh and T.W.B. Kibble, Cosmic Strings, [Rep. Prog. Phys. 58 \(1995\) 477-562](#).  
A. Vilenkin and E.P.S. Shellard, Cosmic Strings and Other Topological Defects, Cambridge University Press, 2000.
- [7] E.B. Bogomol'nyi, The stability of classical solutions, *Sov. J. Nucl. Phys.* 24 (1976) 449-454.
- [8] V. Muñoz-Vitelly, The structure of cosmic strings for a U(1) gauge field related to the conservation of the baryon-number minus lepton-number, M.Sc. thesis, Universidad Nacional Autónoma de México, 2022.
- [9] J.A. García-Hernández, The profile of non-standard cosmic strings, M.Sc. thesis, Universidad Nacional Autónoma de México, 2023.
- [10] V. Muñoz-Vitelly, J.A. García-Hernández and W. Bietenholz, The structure of cosmic strings of a U(1) gauge field for the conservation of  $B - L$ , [Supl. Rev. Mex. Fís. 3 \(2022\) 020713](#).
- [11] A.A. Abrikosov, On the Magnetic Properties of Superconductors of the Second Group, [Soviet Physics JETP 5 \(1957\) 1174](#); The magnetic properties of superconducting alloys, [J. Phys. Chem. Sol. 2 \(1957\) 199](#).
- [12] S. Ducci, P.L. Ramazza, W. González-Viñas and F.T. Arecchi, Order parameter fragmentation after a symmetry-breaking transition, [Phys. Rev. Lett. 83 \(1999\) 5210](#).
- [13] R.P. Feynman, Application of Quantum Mechanics to Liquid Helium, *in* "Progress in Low Temperature Physics", ed. D.F. Brewer, North Holland, Amsterdam 1 (1955) 17-53.
- [14] S.-Z. Lin *et al.*, Topological defects as relics of emergent continuous symmetry and Higgs condensation of disorder in ferroelectrics, [Nat. Phys. 10 \(2014\) 970](#).
- [15] W. Bietenholz and U. Gerber, Berezinskii-Kosterlitz-Thouless Transition and the Haldane Conjecture: Highlights of the Physics Nobel Prize 2016, [Rev. Cub. Fís. 33 \(2016\) 156-168](#).
- [16] R.H. Brandenberger, A.C. Davis and M. Trodden, Cosmic strings and electroweak baryogenesis, [Phys. Lett. B 335 \(1994\) 123-130](#).

- [17] M. James, L. Perivolaropoulos and T. Vachaspati, Detailed stability analysis of electroweak strings, [Nucl. Phys. B 395 \(1993\) 534](#).  
H. Weigel, M. Quandt and N. Graham, Stable charged cosmic strings, [Phys. Rev. Lett. 106 \(2011\) 101601](#).
- [18] W.H. Zurek, Cosmological experiments in superfluid helium?, [Nature 317 \(1985\) 505](#).
- [19] E. Jeong and G.F. Smoot, Search for Cosmic Strings in Cosmic Microwave Background Anisotropies, [Astrophys. J. 624 \(2005\) 21](#).
- [20] M. Wyman, L. Pogosian and I. Wasserman, Bounds on cosmic strings from WMAP and SDSS, [Phys. Rev. D72 \(2005\) 023513](#) [Erratum: [Phys. Rev. D73 \(2006\) 89905\(E\)](#)].
- [21] T. Charnock, A. Avgoustidis, E.J. Copeland and A. Moss, CMB constraints on cosmic strings and superstrings, [Phys. Rev. D 93 \(2016\) 123503](#).
- [22] A. Jelić and L.F. Cugliandolo, Quench dynamics of the 2d XY model, [J. Stat. Mech. Theory Exp. 2011 \(2011\) P02032](#).
- [23] E. López-Contreras, J.F. Nieto Castellanos, E.N. Polanco-Euán and W. Bietenholz, Non-equilibrium dynamics of topological defects in the 3d O(2) model, [PoS LATTICE2023 \(2024\) 346](#).  
J.F. Nieto Castellanos, Topological defects in the O(2) model out of equilibrium, M.Sc. thesis, Universidad Nacional Autónoma de México, 2024.  
E. López-Contreras, Topological defects and the Kibble-Zurek mechanism in the 3d O(2) model, M.Sc. thesis, Universidad Nacional Autónoma de México, 2025.
- [24] H. Fritzsch and P. Minkowski, Unified interactions of leptons and hadrons, [Ann. Phys. \(NY\) 93 \(1975\) 193-266](#).
- [25] W. Buchmüller, C. Greub and P. Minkowski, Neutrino masses, neutral vector bosons and the scale of  $B - L$  breaking, [Phys. Lett. B 267 \(1991\) 395-399](#).
- [26] E.B. Bogomol'nyi and A.I. Vainshtein, Stability of strings in gauge Abelian theory, [Sov. J. Nucl. Phys. 23 \(1976\) 588-591](#).

- [27] L. Jacobs and C. Rebbi, Interaction energy of superconducting vortices, [Phys. Rev. B 19 \(1979\) 4486](#).
- [28] T. Vachaspati and A. Achúcarro, Semilocal cosmic strings, [Phys. Rev. D 44 \(1991\) 3067](#).  
M. Hindmarsh, Existence and stability of semilocal strings, [Phys. Rev. Lett. 68 \(1992\) 1263](#).
- [29] T. Vachaspati, L. Pogosian and D. Steer, Cosmic strings, [Scholarpedia 10 \(2015\) 31682](#).  
L. Sousa, Cosmic strings and gravitational waves, [Gen. Relativ. Gravit. 56 \(2024\) 105](#).
- [30] J.J. Blanco-Pillado, K.D. Olum and X. Siemens, New limits on cosmic strings from gravitational wave observation, [Phys. Lett. B 778 \(2018\) 392-396](#).
- [31] P. Auclair *et al.*, Probing the gravitational wave background from cosmic strings with LISA, [J. Cosmol. Astropart. Phys. 04 \(2020\) 034](#).